

Molecular dynamics simulation of pressure-induced phase transitions in LiYF₄ and LiYbF₄

A. Sen, S. L. Chaplot, and R. Mittal

Solid State Physics Division, Bhabha Atomic Research Centre, Trombay, Mumbai 400 085, India

(Received 13 November 2002; revised manuscript received 29 April 2003; published 8 October 2003)

To take stock of how the laser-host BCT scheelites—viz., LiYF₄ and LiYbF₄—having ambient space group of $I4_1/a$ ($Z=4$), transform structurally with the mere induction of pressure, we resort to pursuing detailed molecular dynamics simulations over a wide range of pressure (0–100 GPa). In carrying out the simulation, we have made use of a well-tested semiempirical interatomic potential around a satisfyingly large periodic macrocell ($4a \times 4b \times 2c$). Our calculated results fairly subscribe to the available experimental observations in maintaining that these fluoroscheelites (even when undoped) undergo initially (within 10 GPa) a second-order transition to the fergusonitelike phase with slight distortions in the atomic arrangements built up in the process. From our extensive analysis, we observe that the space group of this intermediate phase accounting for dynamical stability throughout the Brillouin zone turns out to be $P2_1/c$, which is eventually in mild contrast to what has recently been interpreted as $I2/a$ [A. Grzechnik *et al.*, Phys. Rev. B **45**, 104102 (2002)]. The reason for this apparent disparity may be manifold. This work, however, attempts at finding those out. Further, the hitherto unidentified second high-pressure polymorph that accompanies it almost immediately (around 16 GPa) is also analyzed and subsequently reported in this paper as the new monoclinic prismatic structure ($P2_1/c$, $a=5.99$ Å, $b=9.68$ Å, $c=3.99$ Å, $\beta=108^\circ$, $Z=4$), which seems to remain stable even at 100 GPa. Unlike in the first phase transition, a distinct discontinuity in the evolution of cell volumes is found to crop up during this isospace-group ($P2_1/c^{\text{fergusonite-like}} \rightarrow P2_1/c^{\text{new monoclinic}}$) phase transformation, reflecting it to be of the first-order kind.

DOI: 10.1103/PhysRevB.68.134105

PACS number(s): 61.50.Ks, 64.70.Kb, 64.30.+t

I. INTRODUCTION

Molecular dynamics (MD) simulation is frequently adjudged as a preferential tool in understanding and even in predicting phase transitions of various complex systems under the effect of pressure or temperature. Its spirit of compatibility with the available experimental results followed by its power of far-reaching predictions especially in situations where measurements fail to timely incubate would often invoke in us a torrent of encouragement to go for looking solely at it. With this caveat in mind, we make here an attempt to exploit such a technique for the sake of having a detailed microscopic picture of the complex dynamical phenomena in a well-known laser-host fluoroscheelite system at the atomic level. Recent high-pressure Raman spectroscopic studies¹ have already revealed that pressure induced phase transitions are rather a rule in the scheelite ABO_4 kinds of compounds.

LiYF₄ ($I4_1/a$, $Z=4$), doped with suitable trivalent rare-earth ions (e.g., Nd³⁺, Pr³⁺, Eu³⁺, U³⁺, and so on) is an extensively studied laser material in recent years to meet the ongoing demand in industries. It has essentially a wide-band gap and high crystal field strength (depending on the nature of the dopant) to account² for its superior thermal and optical properties that effectively lead it to host as a wide-range (UV-IR) thermally tunable solid-state laser with remarkably high efficiency. Eyeing the wide gamut of studies on LiYF₄ accomplished over the years,^{3–8,10} we began to develop interest in carrying out phase transitional studies pertaining to this kind of system. Since there is no such phase transition to be reported to date as a function of temperature, LiYF₄ indeed emerges as a promising matrix for a high-pressure investigation.

In the light of the above, we present here an overview of our simulated results upon investigation of the high-pressure phase transformations in LiYF₄ and LiYbF₄. Previously reported high-pressure Raman scattering measurements⁵ indicate a subtle structural anomaly in the ambient fluoroscheelite system at 7 GPa, associated with the lowering of crystal symmetry. In tune with it, our MD simulation also shows the onset of the first phase transition in LiYF₄ at around 6 GPa, followed by a second one near 16 GPa. The crystal thereafter remains as structurally stable even at 100 GPa. We have already observed⁶ that the first phase transition is initiated at the said pressure due to the dynamical instability of a transverse soft acoustic phonon mode at a small wave vector. Recently, Manjon *et al.*,⁷ while executing luminescence measurements on LiYF₄:Eu at room temperature, did come up with strong evidence for a possible phase transformation at a pressure of about 10 GPa, which was further supported by Grzechnik *et al.*,⁸ during their high-pressure x-ray diffraction experiments. We compare our findings with these experimental results of the first phase transition in this paper. However, our predicted structure seems to have a slight distortion compared to that of the fergusonite phase used in interpretation of the experiment.⁸ All the results obtained from our present MD simulation are carefully analyzed and discussed in subsequent sections. We then go on to study the nature of the second phase transition in LiYF₄, for which no clear picture has been made available before. Although there have been signatures of the onset of a second phase transition in the experiment of Grzechnik *et al.*,⁸ the structure of the new phase could not be identified. We are, however, able to determine this second high-pressure polymorph of LiYF₄ through our MD simulation as belonging to a new monoclinic prismatic ($2/m$) class, and its struc-

tural details are subsequently reported in this paper. It is further recorded that unlike the initial phase transition, the second one involves a sharp volume drop along with significant displacements of atoms.

II. SIMULATION

As we intend to study the response of the present fluoroscheelite system upon the induction of external pressure, our obvious goal lies in predicting, as precise as possible, various structural and dynamical changes that occur in the process by cultivating the very idea of molecular dynamics. To carry out the MD simulation, we start with the ambient scheelite structure ($I4_1/a$, $Z=4$) and then slowly allow the system to evolve with time at a constant temperature of 300 K under the condition of different pressures up to 100 GPa. Our model system utilizes a $4\mathbf{a}\times 4\mathbf{b}\times 2\mathbf{c}$ macrocell, where \mathbf{a} , \mathbf{b} , \mathbf{c} are the primitive cell vectors. Since the value of the c parameter in the tetragonal unit cell is approximately twice that of the a parameter, we have taken only half the number of unit cells along the c direction. Each unit cell holds as many as 24 atoms. The size and shape of the unit cell so chosen are treated as variables in the whole process of our simulation. It is important to note that the significant atomic correlations involved here being essentially of short range (<1 nm), a cell size of 768 atoms is overall considered as sufficient for the present MD study. The structure is equilibrated at each pressure for the duration of about 20 ps. Further, the time evolution of the system is calculated at steps of suitable time intervals. For example, we have in the present simulation made use of a time step of only 1 fs, which comes out to be nearly 1/50th of the minimum vibrational period in the system, ensuring thereby the total-energy stability within 1 in 10^6 . Periodic boundary conditions are, however, applied simultaneously around the macrocell to get rid of unwanted surface effects.

For pairwise interactions, the stress tensor $S_{\alpha\beta}$ is expressed as follows⁹:

$$S_{\alpha\beta} = \frac{1}{V} \left[\sum_k m_k v_{k\alpha} v_{k\beta} - \frac{1}{2} \sum_{kk'} \frac{1}{r_{kk'}} \frac{\partial \phi}{\partial r_{kk'}} (r_{kk'})_{\alpha} (r_{kk'})_{\beta} \right]. \quad (1)$$

As usual, α and β represent Cartesian-component indices. On the other hand, k refer to the atoms in the unit cell of volume V while k' designate their neighbors. In the same way, $r_{kk'}$ denominates the interatomic distance between the k th and k' th atom. Further, ϕ denotes the crystal potential and m_k embodies the mass of the atom in the k th sublattice. The pressure function is thus calculated as

$$P = \frac{1}{3} (S_{xx} + S_{yy} + S_{zz}). \quad (2)$$

Temperature is monitored during the simulation process through the total kinetic energy in the macrocell and can thus be changed by suitably scaling the velocities. Similarly, the phase transition is monitored by studying the changes in the structure.

As an essential input to our simulation, we make use of the following well-tested semiempirical interatomic potential^{6,10}

$$\phi = \frac{e^2}{4\pi\epsilon_0} \frac{Z_k Z_{k'}}{r_{kk'}} + A \exp \left[-B \frac{r_{kk'}}{r_k + r_{k'}} \right] - \frac{C}{r_{kk'}^6}. \quad (3)$$

Here, r_k and Z_k refer, respectively, to the effective radius and charge of the k th atom while A , B , and C are constants. The potential function as outlined above comprises a string of three different energy terms related, respectively, to the long-ranged Coulomb type, the short-ranged Born-Mayer type, and finally, the weak but effective van der Waals type interactions. It is rather implicit that these two-body potentials include, to some extent, many-body forces too, as exploited earlier.¹¹ The Ewald technique has been employed in the present MD simulation so as to integrate the two-body Coulomb interactions, while the other two potential terms being of short-range order are directly summed up over all pairs of atoms up to 7 Å separation.

III. RESULTS

A. Phase transition I (scheelite to fergusonite-like)

By way of our MD simulation (at 300 K) as a function of pressure in the ambient fluoroscheelite system under study, we initially come across what would be in an apparent manner a second order phase transition in both LiYF_4 and LiYbF_4 , at around 6 GPa and 5 GPa, respectively, with no significant volume drop observed in the process (Figs. 1 and 2). Following the convention in the literature,⁸ there is a relabeling of the unit-cell axes across the first transition from a, b, c to c, a, b , respectively. The bifurcations in the lattice parameters of LiYF_4 and LiYbF_4 clearly demonstrate distortions in the tetragonal scheelite structure, leading to the onset of an initial phase transition in the system. The resulting structure is very close to the well-known fergusonite phase. The angle β , which gives a measure of the monoclinic distortion in the system, turns out to be around 98° for LiYF_4 at about 13 GPa (Table I). A quantitative comparison of the experimentally observed⁸ and our simulated bond lengths in this high-pressure phase polymorph of LiYF_4 shows further a considerably fair agreement.

The fractional atomic coordinates along the three crystallographic directions, as obtained out of our MD simulation for the chosen unit cell in any of the transformed phases, provide insight into the possible structures of that new phase polymorph. Hence, we begin with an extensive analysis for determining the first high-pressure phase of LiYF_4 . As already noted by Grzechnik *et al.*,⁸ this phase is identified as fergusonite with the space group of $I2/a$ ($Z=4$). However, our MD simulation reveals that the space group of the new phase is rather close to $P2_1/c$ ($Z=4$). Thus to confirm the dynamically most favored structure, we go on investigating the dynamical stability of LiYF_4 with both the possible space groups. To implement it, we carry out complementary lattice dynamical calculations in which the total energy is minimized with respect to the structural variables constrained only by the space-group symmetry. Analysis is made sepa-

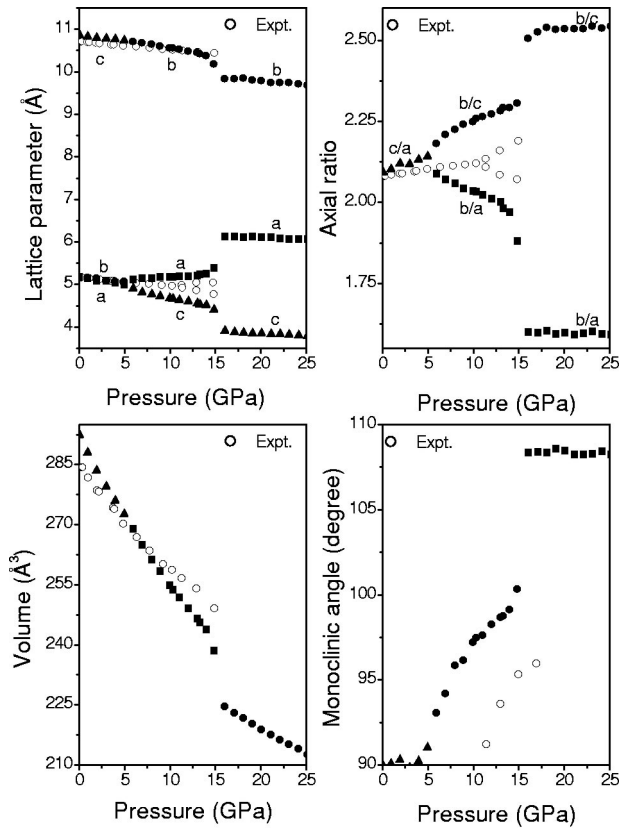


FIG. 1. Pressure dependence of lattice parameters for scheelite, fergusonitelike and the new monoclinic phases of LiYF_4 up to 25 GPa. The measured high-pressure x-ray diffraction data [Grzechnik *et al.*, (Ref. 8)] are shown by the open circles, while the solid ones represent our simulated results.

rately for the two space groups $I2/a$ and $P2_1/c$. Figure 3 gives a qualitative impression of the better stability of the $P2_1/c$ space group in terms of the crystal potential energy over the experimentally determined $I2/a$, in the low-temperature region (approaching 0 K). Further, unlike for $I2/a$, we get all positive real phonon frequencies in the entire

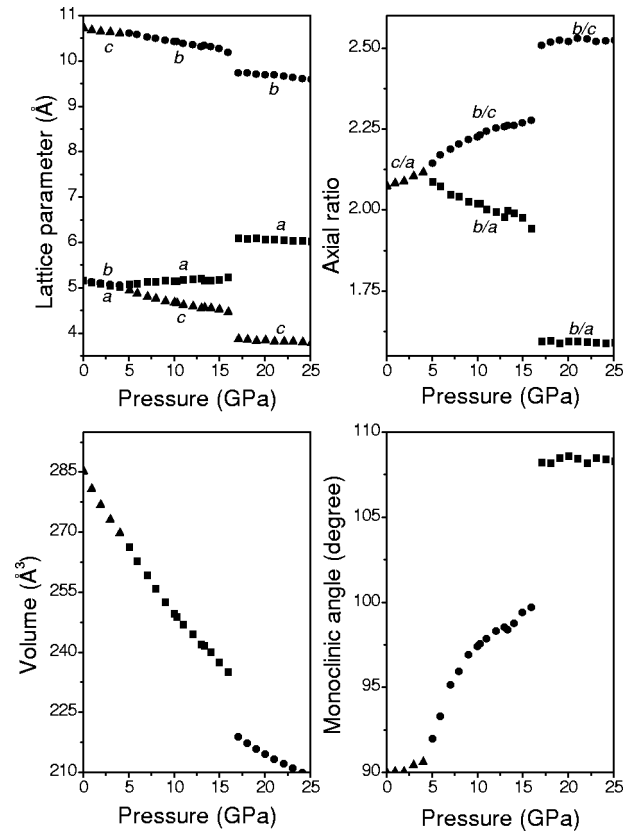


FIG. 2. A simulated picture on the pressure dependence of lattice parameters in LiYbF_4 up to 25 GPa, elucidating all its three high-pressure phases.

Brillouin zone only for the space group $P2_1/c$, validating our simulated space group as the configurationally preferred structure (within the same low-temperature limit). Moreover, in order to confirm this picture, we extend the simulation of this $P2_1/c$ structure above 300 K and indeed find that the simulated structure at 400 K corresponds to the coveted $I2/a$ space group. Table I gives the detail of the structural param-

TABLE I. A comparison between the experimental (Ref. 8) and the simulated structural parameters of the first high-pressure modification of LiYF_4 . The maximum atomic shift associated with the simulated space groups (viz., $P2_1/c$ and $I2/a$) under different temperatures (viz., 300 K and 400 K) is 0.16 Å.

	Fergusonitelike phase of LiYF_4								
	Experimental $I2/a$, $Z=4$ ($P=13.3$ GPa)			Calculated $P2_1/c$, $Z=4$ ($P=13.3$ GPa, $T=300$ K)			Calculated $I2/a$, $Z=4$ ($P=13.3$ GPa, $T=400$ K)		
$a(\text{Å})$	5.0416			5.22			5.25		
$b(\text{Å})$	10.4174			10.43			10.43		
$c(\text{Å})$	4.7808			4.57			4.56		
β (deg)	95.279			98.6			98.7		
Atom	x	y	z	x	y	z	x	y	z
Li	0.25	0.362	0	0.253	0.327	0.997	0.25	0.325	0
Y	0.25	0.879	0	0.253	0.885	0.014	0.25	0.885	0
F(1)	0.430	0.0317	0.756	0.388	0.041	0.763	0.388	0.048	0.777
F(2)	0.937	0.2962	0.136	0.945	0.298	0.157	0.958	0.293	0.186
F(3)				0.888	0.553	0.288			
F(4)				0.472	0.787	0.717			

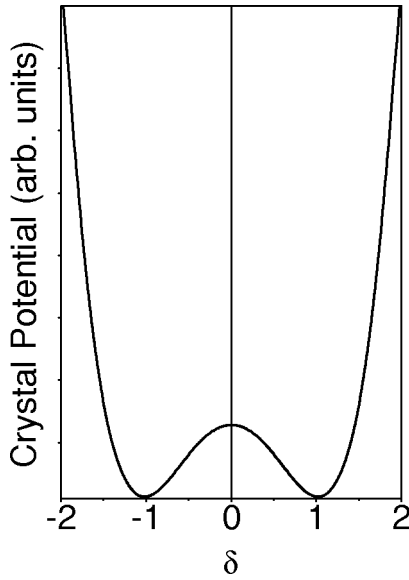


FIG. 3. Variation in the potential energy per unit cell of LiYF_4 as a function of distortion (δ) of the fergusonitelike structure in the simulated space group of $P2_1/c$ from the experimentally determined space group of $I2/a$. Here, $\delta=0$ and $\delta=1$ refer to the atomic coordinates in the two space groups—viz., $I2/a$ and $P2_1/c$, respectively—at their respective potential minimum.

eters at this temperature. We observe that the atomic shifts in going from $P2_1/c$ to $I2/a$ fergusonitelike structure are below 0.2 \AA , which is rather quite small. Further, we compare the experimental and calculated structure factors in Table II, a detailed overview of which is subsequently illustrated in Fig. 4. Due to the different space groups of our calculated structure, several reflections acquire small but finite intensities which, however, remain absent from the space group used in the experimental data analysis.⁸

B. Phase transition II (fergusonitelike to new monoclinic)

While continuing our MD simulation to higher pressures up to 100 GPa, we encounter another structural phase transition in the same system. This second transition seems to occur in LiYF_4 in the vicinity of 16 GPa and in LiYbF_4 , about 17 GPa. Unlike in the previous case, we observe here a significant volume drop, which is nearly 6% for LiYF_4 and 7% for LiYbF_4 . As is seen from Figs. 1 and 2, discontinuities crop up in the angle of monoclinic distortion (β) as well. This second phase transition is, therefore, clearly of the first order. The angle β turns out here to be 108° for LiYF_4 at the transition pressure (Table III) and then continues to remain stable even at 100 GPa (Fig. 5). Owing to the transition from fergusonitelike structure to this new monoclinic phase, the a parameter increases by about 15% while the other two lattice parameters (viz., b and c) decrease, respectively, by 7% and 13%. The angle β is also up by 10%. From the analysis of our simulated results, we notice that this high-pressure new phase polymorph is actually another kind of monoclinic structure with the prismatic class ($2/m$). We determine its space group to be $P2_1/c$ ($Z=4$), as enumerated in Table III. For conviction, we further carry out lattice dynamical calcu-

TABLE II. A comparison of the observed (Ref. 8) and the calculated structure factors (in arb. units) for d_{hkl} values for the first 20 reflections in the initial high-pressure phase of LiYF_4 at 13.3 GPa and 300 K. The isotropic temperature factor $B_{iso}(=8\pi^2\langle u^2 \rangle/3)$ values we have used here are 0.92, 0.64, 0.90, 1.08, 0.95, and 0.90 \AA^2 for the Li, Y, F(1), F(2), F(3), and F(4) atoms, respectively, as estimated from our calculation. The calculated space group of this fergusonitelike phase in the low-temperature limit is $P2_1/c$, while that of the experimental one is $I2/a$ (see the text for details).

h	k	l	d_{hkl}		$ F_{hkl} ^2$	
			Expt.	Calc.	Expt. $I2/a, Z=4$	Calc. $P2_1/c, Z=4$
0	2	0	5.21	5.22	15	16
1	0	0	5.02	5.16	0	2
1	1	0	4.52	4.63	1391	1043
0	1	1	4.33	4.15	864	1354
1	2	0	3.62	3.67	0	0
0	2	1	3.52	3.42	0	10
1	1	-1	3.43	3.48	0	6
1	1	1	3.15	3.04	0	13
1	2	-1	2.98	3.01	2098	2052
1	3	0	2.86	2.88	520	576
0	3	1	2.81	2.76	331	225
1	2	1	2.79	2.71	1832	2034
0	4	0	2.61	2.61	630	718
2	0	0	2.51	2.58	557	718
1	3	-1	2.52	2.53	0	0
2	1	0	2.44	2.51	0	0
1	3	1	2.39	2.34	0	53
0	0	2	2.38	2.26	640	320
0	1	2	2.32	2.21	0	0
1	4	0	2.31	2.33	0	8

lation of the normal modes in this system and observe that $P2_1/c$ indeed represents a dynamically stable configuration for this new phase. As the Table III demonstrates, Li atoms are surrounded by eight fluorine atoms with six of them having an average bond length of about 2 \AA and the remaining two of 2.7 \AA (Table III). On the other hand, for the rare-earth yttrium atoms, ten fluorine atoms are found to close in at distances ranging from 2.13 to 2.42 \AA .

IV. DISCUSSIONS

Two distinct high-pressure phase transitions are observed in both LiYF_4 and LiYbF_4 , one being apparently of second order while the other of the first order kind, as enumerated in Tables I and III. On looking at the crystal structures accounting for all the three phases of LiYF_4 , as depicted in Fig. 6, we come across significant nearest-neighbor atomic displacements in case of Li atoms in transforming from scheelite to fergusonitelike phase (average 0.5 \AA) and also from fergusonitelike to the new monoclinic phase (more than 1 \AA). This is also well manifested in our further calculations of pair-

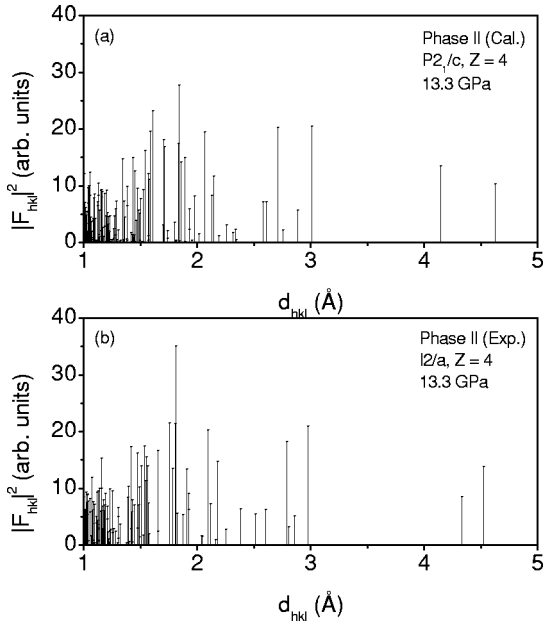


FIG. 4. Graphical layout of (a) calculated and (b) experimental [Grzechnik *et al.* (Ref. 8)], structure factor patterns for the fergusonitlike phase in LiYF_4 at 13.3 GPa. Multiplicity factor has not been included here.

correlation functions for the constituent atoms, as a function of the interatomic distance $r_{kk'}$.

From the bond angle distributions involving the first nearest neighbors of Li-F and Y-F, we find that the F-Li-F and Li-F-Y angles display a sharp decline, while their distributions broaden across the scheelite to fergusonitlike transition. However, during the second phase transition, the bond angle distributions of F-Y-F cater to a substantial lowering in angles associated with increased coordinations.

From the graphical representations of scheelite to fergusonitlike and also of the subsequent second phase transition in LiYF_4 as well as in LiYbF_4 (Figs. 1 and 2), we get an idea of how the structural changes occur in these two compounds upon induction of pressure. Our simulated diffraction diagrams for LiYF_4 at 300 K under different pressures are shown in Fig. 7. Associated peak splitting along with the introduction of some additional weak reflections is distinctly observed in the present simulation, indicating the actual occurrence of pressure-induced phase transitions in the system. However, the calculated intensities may not be found to match very well with those of the experiment,⁸ due likely to the preferred orientations of the powder sample utilized in the latter.

As mentioned earlier, Raman scattering measurements at 300 K by Sarantopoulou *et al.*,⁵ indicate a possible onset of structural phase transition in LiYF_4 near 7 GPa. On the other hand, the present MD simulation suggests the initiation of the phase transition in the same compound at about 6 GPa. Recently, the luminescence measurements made by Manjon *et al.*,⁷ indicate that slight changes in the scheelite structure occur around 5.5 GPa and discontinuous changes near 10 GPa. However, the subsequent high-pressure x-ray diffraction experiment carried out by Grzechnik *et al.*,⁸ advocates

TABLE III. Structural parameters of the second high-pressure monoclinic polymorph ($P2_1/c$, $Z=4$) of LiYF_4 on potential minimization of the simulated structure ($P=18$ GPa, $T=0$ K). Here, $a=5.99$ Å, $b=9.68$ Å, $c=3.99$ Å, $\beta=108^\circ$, $V=221.6$ Å³. Positional parameters are listed in the upper part while the bottom part enumerates the selected interatomic distances (not exceeding 3.0 Å) in the crystal structure of the second high-pressure modification of LiYF_4 .

Atom	Site	x	y	z		
Li	4e	0.783	0.796	0.819		
Y	4e	0.726	0.403	0.863		
F(1)	4e	0.887	0.603	0.937		
F(2)	4e	0.637	0.525	0.336		
F(3)	4e	0.116	0.674	0.540		
F(4)	4e	0.499	0.705	0.880		
Ion pair	No.	Distance	Ion pair	No.	Distance	
Li-F(1)		1.94	F(1)-F(1)	2	2.47	
		2.82	F(1)-F(2)		2.47	
Li-F(2)		1.97			2.49	
		2.06			2.51	
		2.54	F(1)-F(3)		2.37	
Li-F(3)		1.94	F(1)-F(4)		2.30	
Li-F(4)		1.99			2.82	
		2.03	F(2)-F(2)		2.36	
Y-F(1)		2.23	F(2)-F(3)		2.52	
		2.38			2.61	
		2.39	F(2)-F(4)		2.47	
Y-F(2)		2.13	F(3)-F(3)		2.44	
		2.21			2.72	
		2.18	F(3)-F(4)		2.42	
Y-F(3)		2.32			2.46	
		2.42			2.74	
		2.19	F(4)-F(4)		2.17	
Y-F(4)		2.36				
		2.36				
Li-Li	2	2.18				

for the initial phase transition occurring at 10.6 GPa. We would mention that although LiYF_4 does not distort as CaWO_4 lattice does at high dopant,¹² which is also clear from our simulation when we compare the equation of states for both LiYF_4 and LiYbF_4 , the reason for the apparent inequality in our transition pressure calculation lies perhaps in the limitation of exploiting a semiempirical potential^{6-8,10} to accomplish the simulation. It is, however, worthy to emphasize here that our intention in carrying out the present MD simulation was primarily to have a rather qualitative overview of possible high-pressure phase transitions in ternary halides: viz., LiYF_4 and LiYbF_4 . Our analysis establishes that the initial high-pressure modification of LiYF_4 is associated with a continuous increase of the monoclinic distortion of the crystal until the second one is encountered (Fig. 1), which is in tune with the experimental observations.^{7,8} As Fig. 2 demonstrates, we come across a similar kind of behavior in LiYbF_4 too.

We observe that although in the low-temperature limit

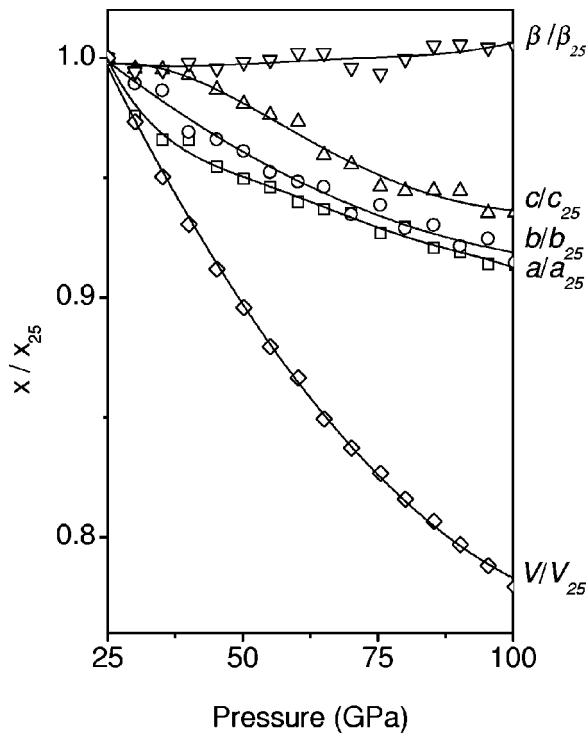


FIG. 5. An overview of the simulated equations of state for LiYF_4 in the new monoclinic phase, up to 100 GPa. The lines are guide to the eye through the simulated data symbols. The lattice constants and volume have been normalized by their respective values at 25 GPa as given in Fig. 1.

(0–300 K) the simulated space group of the first high-pressure phase is close to $P2_1/c$, as soon as the system overcomes the energy barrier (Fig. 3) upon heating, the dynamically stable space group turns out to be $I2/a$, tallying the experimental observations.⁸ This is not much unusual in the sense that a similar kind of behavior is also encountered in clinopyroxenes with the pigeonite structure, where it has been observed¹³ that high-temperature pigeonite possesses the space group of $C2/c$, while low-temperature pigeonite has $P2_1/c$ as its space group.

So far as the second high-pressure phase of LiYF_4 is concerned, we observe that there are six Li-F bonds of approximately 2 Å length, accounting for the six-coordinated bonding of Li cations in the system. The Li-F coordination thus changes from tetrahedral to octahedral (LiF_4 to LiF_6) at high pressure, in going from fergusonite to the new monoclinic structure. In some ABO_4 kinds of compounds—viz., CdWO_4 —where the highly distorted edge-shared BO_6 units are found to be present at high pressure in the wolframite phase, the W-O coordination turns out to be octahedral.¹⁴ The polymorphic transformation of LiYF_4 from the fergusonitelike phase into a modified monoclinic one may thus be understood from the higher atomic packing in the latter one. In this context, we note that NdTaO_4 shows¹⁵ a phase transition from fergusonite to the monoclinic LaTaO_4 -type structure at high pressure. Both LaTaO_4 and the high pressure modification of NdTaO_4 have TaO_6 octahedra with a similar Ta-O bond length as in LiF_6 octahedra. On the other hand, while the rare-earth yttrium cations form ten short bonds to

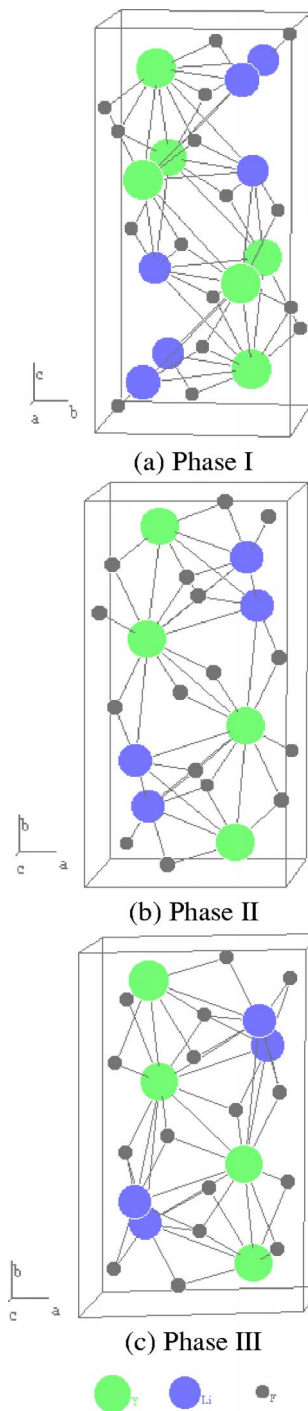


FIG. 6. Simulated high-pressure structures in (a) scheelite, (b) fergusonitelike, and (c) the new monoclinic phases of LiYF_4 ; the circles depicting the three constituent atoms (viz., Y, Li, and F) are in decreasing order of size.

fluorine anions at distances varying between 2.13 Å and 2.42 Å with an average of about 2.3 Å, the lanthanum cations are found to be eight coordinated with oxygen anions. With a view to Shannon *et al.*,¹⁶ the tenfold coordination of Y cations is mainly due to greater Y-F bond strength. Since the size and charge of Y and La are roughly alike, it is the higher electronegativity of Y cations (and also of F anions) which

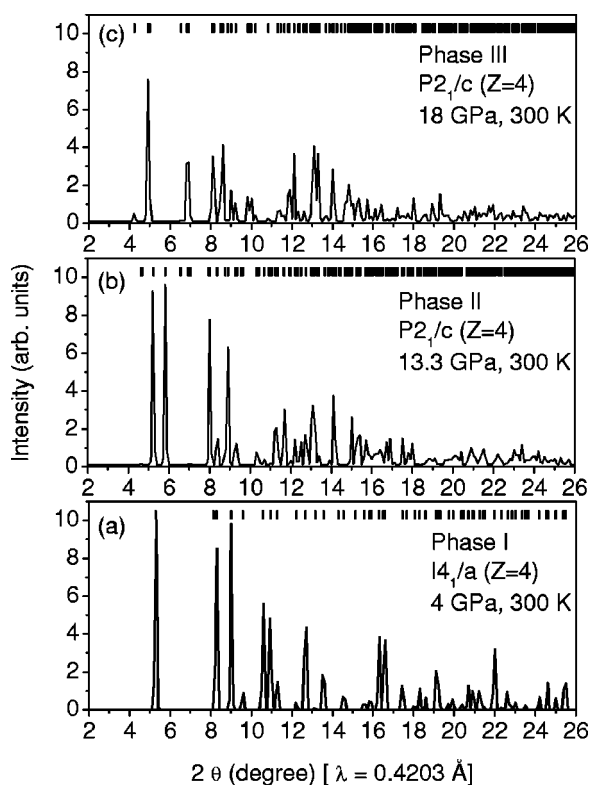


FIG. 7. Simulated diffraction patterns for the scheelite ($I4_1/a$, $Z=4$), fergusonite-like (see text, $P2_1/c$, $Z=4$), and the new monoclinic ($P2_1/c$, $Z=4$) phases of LiYF_4 at the respective pressures as mentioned. Vertical markers indicate Bragg reflections.

contribute to the greater Y-F bond strength resulting in a higher coordination number. Hence, even though there is not much information on the pressure-induced post-fergusonite phases in ternary oxides¹⁷ as well as in ternary halides, the second high-pressure modification of LiYF_4 is found to be apparently close to LaTaO_4 kind of structure ($P2_1/c$, $a = 7.59 \text{ \AA}$, $b = 5.46 \text{ \AA}$, $c = 7.7 \text{ \AA}$, $\beta = 100.03^\circ$, $Z = 4$) with, however, different lattice parameters.

V. CONCLUSIONS

Based on a simple (though realistic) interatomic potential across a limited-sized macrocell, the present molecular dy-

namics study allows us to satisfyingly reproduce the initial high-pressure phase analog of the ambient fluoroscheelite, LiYF_4 , in favor of the fergusonite-like structure and also subsequently predict its hitherto unidentified second new-phase polymorph at higher pressures as pertaining to a close-packed monoclinic prismatic class. Notwithstanding, an ambiguity that once clouded at the outset around making the choice of the proper space group to represent the dynamically stable first high-pressure modification of LiYF_4 has finally been repulsed off in the process of our extensive analysis on further accomplishment of the energy minimization and lattice dynamical calculations. Moreover, we have been able to observe through our MD simulation that the second high-pressure monoclinic prismatic phase involving an octahedral coordination around the Li cation remains stable even at 100 GPa. This iota of information is otherwise subverted by experimental limitations. Further, our simulation has made it also possible to shed light on the pressure-induced phase transitional behavior in another similar kind of compound: viz., LiYbF_4 . Our simulated results thus enable a microscopic visualization of the nature and pathways of the structural changes that occur at high pressures and provide this way a deeper understanding of the underlying dynamical phenomena in the ambient fluoroscheelite system.

Finally, although the present MD simulation suggests no more structural phase transition to take place above 16 GPa in LiYF_4 , it might yet appear to be quite interesting in tracing out whether there occurs any further anomaly in the system on substantially increasing the temperature as well along with the pressure, since scheelites (e.g., RNbO_4 , RTaO_4 , etc., with $R = \text{La to Lu}$) are quite known¹⁸ to be among the few rare systems to undergo pure and proper ferroelastic phase transitions with temperature.

ACKNOWLEDGMENTS

A.S. would like to express his deep sense of gratitude towards the Council of Scientific and Industrial Research (CSIR), India, for rendering necessary financial support throughout the work and gratefully acknowledges as well the continuous encouragement and care taken by Dr. S. K. Sikka and Dr. M. Ramanadham during this period.

¹A. Jayaraman, B. Batlogg, and L. G. van Uiter, *Phys. Rev. B* **28**, 4774 (1983); **31**, 5423 (1983); A. Jayaraman, G. A. Kourouklis, L. G. van Uiter, W. H. Grodkiewicz, and R. G. Maines, Sr., *Physica A* **156**, 325 (1988); D. Christofilos, G. A. Kourouklis, and S. Ves, *J. Phys. Chem. Solids* **56**, 1125 (1995); S. R. Shieh, L. C. Ming, and A. Jayaraman, *ibid.* **57**, 205 (1996).
²J. L. Adam, W. A. Sibley, and D. R. Gabbe, *J. Lumin.* **33**, 391 (1985); C. K. Jayasankar, M. F. Reid, and F. S. Richardson, *Phys. Rev. B* **155**, 559 (1989).
³S. A. Miller, H. E. Rasty, and H. H. Caspers, *J. Chem. Phys.* **52**, 4172 (1970); E. Garcia and R. R. Ryan, *Acta Crystallogr., Sect.*

C: Cryst. Struct. Commun. **49**, 2053 (1993); P. Rogin and J. Hulliger, *J. Cryst. Growth* **179**, 551 (1997); S. Salaün, M. T. Fornoni, A. Bulou, M. Rousseau, P. Simon, and J. Y. Gesland, *J. Phys.: Condens. Matter* **9**, 6941 (1997).
⁴S. Salaün, A. Bulou, M. Rousseau, B. Hennion, and J. Y. Gesland, *J. Phys.: Condens. Matter* **9**, 6957 (1997).
⁵E. Sarantopoulou, Y. S. Raptis, E. Zouboulis, and C. Raptis, *Phys. Rev. B* **59**, 4154 (1999).
⁶A. Sen, S. L. Chaplot, and R. Mittal, *J. Phys.: Condens. Matter* **14**, 975 (2002).
⁷F. J. Manjon, S. Jandl, K. Syassen, and J. Y. Gesland, *Phys. Rev.*

- B **64**, 235108 (2001).
- ⁸A. Grzechnik, K. Syassen, I. Loa, M. Hanfland, and J. Y. Gesland, Phys. Rev. B **65**, 104102 (2002).
- ⁹M. P. Allen and D. J. Tildesley, *Computer Simulation of Liquids* (Clarendon, Oxford, 1987).
- ¹⁰A. Sen, S. L. Chaplot, and R. Mittal, Phys. Rev. B **64**, 024304 (2001).
- ¹¹S. L. Chaplot, Phase Transitions **19**, 49 (1989); S. L. Chaplot and S. K. Sikka, Phys. Rev. B **47**, 5710 (1993); S. L. Chaplot and S. K. Sikka, *ibid.* **61**, 11 205 (2000); S. L. Chaplot and N. Choudhury, Am. Mineral. **86**, 752 (2001).
- ¹²M. R. Brown, K. G. Roots, and W. A. Shand, J. Phys. C **2**, 593 (1969).
- ¹³P. Robinson, Malcolm Ross, G. L. Nord, Jr., J. R. Smyth, and H. W. Jaffe, Am. Mineral. **62**, 857 (1977).
- ¹⁴A. Jayaraman, S. Y. Wang, and S. K. Sharma, Phys. Rev. B **52**, 9886 (1995).
- ¹⁵Y. A. Titov, A. M. Sych, A. N. Sokolov, A. A. Kapshuk, V. Ya. Markiv, and N. M. Belyavina, J. Alloys Compd. **311**, 252 (2000).
- ¹⁶R. D. Shannon, J. Chenavas, and J. C. Joubert, J. Solid State Chem. **12**, 16 (1975).
- ¹⁷O. Fukunaga and S. Yamaoka, Phys. Chem. Miner. **5**, 167 (1979).
- ¹⁸A. Pinczuk, Gerald Burns, and F. H. Dacol, Solid State Commun. **24**, 163 (1977); A. Pinczuk, B. Welber, and F. H. Dacol, *ibid.* **29**, 515 (1979); M. Wada, Y. Nakayama, A. Sawada, S. Tsunekawa, and Y. Ishibashi, J. Phys. Soc. Jpn. **47**, 1575 (1979); W. L. F. David and A. M. Glazer, Phase Transitions **1**, 155 (1979); Gu Benuyan, M. Copic, and H. Z. Cummins, Phys. Rev. B **24**, 4098 (1981).